

Topologically disordered systems at the glass transition

This article has been downloaded from IOPscience. Please scroll down to see the full text article.

2006 J. Phys.: Condens. Matter 18 11507

(<http://iopscience.iop.org/0953-8984/18/50/007>)

View [the table of contents for this issue](#), or go to the [journal homepage](#) for more

Download details:

IP Address: 129.252.86.83

The article was downloaded on 28/05/2010 at 14:53

Please note that [terms and conditions apply](#).

Topologically disordered systems at the glass transition

Michael I Ojovan¹ and William E Lee²

¹ Immobilisation Science Laboratory, Department of Engineering Materials,
University of Sheffield, UK

² Department of Materials, Imperial College London, UK

E-mail: M.Ojovan@sheffield.ac.uk and W.E.Lee@imperial.ac.uk

Received 28 July 2006, in final form 30 October 2006

Published 27 November 2006

Online at stacks.iop.org/JPhysCM/18/11507

Abstract

The thermodynamic approach to the viscosity and fragility of amorphous oxides was used to determine the topological characteristics of the disordered network-forming systems. Instead of the disordered system of atoms we considered the congruent disordered system of interconnecting bonds. The Gibbs free energy of network-breaking defects (configurons) was found based on available viscosity data. Amorphous silica and germania were used as reference disordered systems for which we found an excellent agreement of calculated and measured glass transition temperatures. We reveal that the Hausdorff dimension of the system of bonds changes from Euclidian three-dimensional below to fractal 2.55 ± 0.05 -dimensional geometry above the glass transition temperature.

(Some figures in this article are in colour only in the electronic version)

1. Introduction

The distribution of atoms and molecules in amorphous materials is irregular and is described as topologically disordered in that an amorphous material cannot be produced by continuously distorting a crystalline lattice. There is an enormous diversity of amorphous materials, including: covalently bonded oxide glasses such as vitreous silica, the structure of which is modelled by a continuous random network of bonds (network-forming materials); metallic glasses bonded by isotropic pair potentials, whose structure is thought of as a dense random packing of spheres; and amorphous polymers, whose structure is understood to be an arrangement of interpenetrating random-walk-like coils strongly entangled with each other. Amorphous materials can be in two forms: either as viscous liquids or glasses. A glass is a disordered material like a viscous liquid but which behaves mechanically like an isotropic solid. Although fundamentally important, the nature of the glassy state is not well understood, neither for ordinary glasses such as vitreous oxides nor for spin glasses [1, 2]. Moreover it is recognized that the theory of ordinary glasses may suffer from a lack of commonly

accepted simplified models analogous to that of spin glasses such as the Edwards–Anderson model [2]. A glass is most commonly formed by cooling a viscous liquid fast enough to avoid crystallization. Practically any liquid crystallizes if the cooling rate is sufficiently slow, hence there is a critical cooling rate above which a liquid can be vitrified. On cooling the viscosities of liquids gradually increase and the liquid–glass transition is often regarded as a transition for practical purposes rather than a thermodynamic phase transition [3]: by general agreement it is considered that a liquid on being cooled becomes a glass when the viscosity equals 10^{12} Pa s (10^{13} poise) or where the relaxation time is 10^2 s [3, 4]. The liquid–glass transition is accompanied by spectacular changes in physical properties (e.g. glasses are rigid whereas supercooled liquids are soft); however, no obvious changes occur at the molecular level and the material is topologically disordered both in liquid and glassy states [5]. However, at the glass transition temperature, T_g , rearrangements occur in an amorphous material so that the T_g can be exactly detected by analysing, for example, the behaviour of derivative parameters such as the coefficient of thermal expansion or the specific heat [6]. As a result the glass transition is considered as a second order phase transition in which a supercooled melt yields, on cooling, a glassy structure and properties similar to those of crystalline materials, e.g. of an isotropic solid material [7]. The theory of second order phase transitions describes the temperature behaviour of the specific heat (C_p) near T_g by the power law $C_p(T) \propto 1/|T - T_g|^\alpha$, where α is the universal critical exponent [8]. The specific heat of either a supercooled liquid or an equilibrium melt $C_{p,\text{liquid}}(T)$ is higher than that of a glass $C_{p,\text{glass}}(T)$, the thermal expansion coefficient of a liquid $\alpha_{\text{liquid}}(T)$ is higher than that of a glass $\alpha_{\text{glass}}(T)$, and the isothermal compressibility of a liquid κ_{liquid} is higher than that of a glass κ_{glass} . The differences in specific heat ΔC_p , thermal expansion coefficient $\Delta\alpha$ and isothermal compressibility $\Delta\kappa$ at second order phase transitions obey two Ehrenfest theorems $\Delta C_p = T(dP/dT)\Delta\alpha$ and $\Delta\alpha = \Delta\kappa(dP/dT)$, where P is pressure [8]. Indeed at the liquid–glass transition the two Ehrenfest theorems for the pressure dependence of transition temperature dT_g/dP are approximately obeyed [9]. Although kinetic approaches enable justification of these theorems [9] the glass transition shows distinctly thermodynamic phase transition features [7, 10]. However, being a kinetically controlled phenomenon the liquid–glass transition exhibits a range of T_g which depends on the cooling rate with maximal T_g at highest rates of cooling [6]. Thus the liquid–glass transition has features in common with both second order thermodynamic phase transitions and those of kinetic origin [6, 8].

Liquid–glass transition phenomena are observed universally in various types of liquids, including molecular liquids, ionic liquids, metallic liquids, oxides and chalcogenides [11–15]. There is no long range order in amorphous materials; however, at the liquid–glass transition a kind of freezing transition occurs which is similar to that of second order phase transitions and which it may be possible to characterize using an order parameter [2]. In addition, because the ordered system (and the glass state seems to be more ordered than the liquid one) has a higher symmetry, the question of the symmetry arises for disordered systems at the liquid–glass transition [2]. The general theoretical description of the topologically disordered glassy state focuses on tessellations [16] and is based on partitioning space into a set of Voronoi polyhedrons filling the space of a disordered material. A Voronoi polyhedron is a unit cell around each structural unit (atom, defect, group of atoms) which contains all the points closer to this unit than to any other and is an analogue of the Wigner–Seitz cell in crystals [3]. For an amorphous material the topological and metric characteristics of the Voronoi polyhedron of a given unit are defined by its nearest neighbours so that its structure may be characterized by a distribution of Voronoi polyhedrons. Considerable progress has been achieved in investigating the structure and distribution of Voronoi polyhedrons of amorphous materials using molecular dynamic (MD) models [17–20]. MD simulations reveal that the difference between a liquid

and glassy state of an amorphous material is caused by the formation of percolation clusters in the Voronoi network: namely in the liquid state low density atomic configurations form a percolation cluster whereas such a percolation cluster does not occur in the glassy state [17, 20]. The percolation cluster made of low density atomic configurations is called a liquid-like cluster as it occurs only in a liquid and does not occur in the glassy state. Nonetheless, a percolation cluster can be envisaged in the glassy state but formed by high density configurations [17, 18]. Solid-like percolation clusters made of high density configurations seem to exist in all glass phase models of spherical atoms and dense spheres [17, 18]. Thus MD simulations demonstrate that near T_g the interconnectivity of atoms (e.g. the geometry of bonds) changes due to the formation of percolation clusters composed of coordination Voronoi polyhedrons. While these percolation clusters made of Voronoi polyhedrons are more mathematical descriptors than physical objects their formation results in changes in the derivative properties of materials near the T_g [18]. The liquid–glass transition is thus characterized by a fundamental change in the bond geometries so that this change can be used to distinguish liquids from glasses although both have amorphous structures [17, 21].

The purpose of this work is to analyse the disordered structure of bonds and the spatial distribution of defects which break the net of bonds of an amorphous material with temperature. We used for numerical analysis two binary systems—amorphous silica and germania—as the simplest glass-forming materials. Thermodynamic data for broken bonds were evaluated based on recent results on the viscosity of amorphous materials treated theoretically by use of Doremus’ defect model of viscosity [22–24]. This model relates the viscosity of an amorphous material to the concentration of broken bonds (defects) which are believed to be responsible for the viscous flow [22]. Given some known thermodynamic parameters of point defects, analytical evaluation of their concentration becomes feasible (including in high concentration areas) as does determination of temperature ranges where dynamic percolation clusters made of broken bonds are formed [21, 25, 26].

Recognition of the role of interconnectivity of the microscopic elements of disordered systems and application of percolation theory has enabled the development of the statistical physics of disordered systems [26]. Amorphous materials have no elementary cell characterized by a certain symmetry, which can reproduce the distribution of atoms by its infinite repetition. Instead the symmetry of a topologically disordered system is characterized by the Hausdorff dimension of interconnecting and broken bonds. Two types of topological disorder characterized by different symmetries can be revealed in an amorphous material based on the analysis of broken bond concentrations: (i) three-dimensional (3D) (Euclidean), which occurs at low temperatures when no percolation clusters are formed and the geometrical structures of bonds can be characterized as 3D with no preferential pathways of motion and (ii) $d_f = 2.55 \pm 0.05$ -dimensional (fractal), which occurs at high temperatures when percolation clusters made of broken bonds are formed and the geometries of the structures formed can be characterized as fractal objects with preferential pathways for defect (broken bond) motion. Similarly to MD results [17, 18] we revealed that the geometry of bonds changes at T_g : the distribution of net defects is Euclidean below T_g but becomes fractal above it due to the formation of dynamic percolation clusters made of broken bonds. The glassy state is characterized by a Euclidean 3D distribution of bonds and the liquid state is characterized by a fractal 2.55 ± 0.05 -dimensional distribution. Our results are consistent with results of MD models and reflect the same change of the geometry of atomic distribution in amorphous materials at T_g , namely the change of the symmetry of distribution. Thus the transition from a glassy to a supercooled liquid state can be treated as a change in the symmetry of topological disorder. This makes the liquid–glass transition similar to second order thermodynamic phase transitions in crystalline materials which are always characterized by symmetry changes [8].

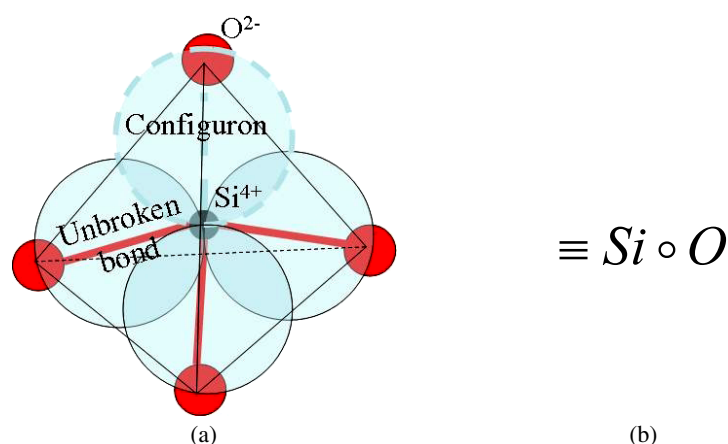


Figure 1. Configurational unit of amorphous silica (tetrahedron $[\text{SiO}_4]$), its bond model and designation. (a) Bond model shown with three unbroken bonds and one configuron. (b) Bond model designation.

2. Formation of network-breaking defects

Binary oxide systems that form network glasses are of significant scientific and technological importance and there is a need for a detailed knowledge of their structure. However, for the disordered atomic arrangement which occurs in amorphous materials a precise structure description over a wide range of length scales is notoriously difficult to obtain. The atomic sites form a topologically disordered network, and the presence of two chemical species adds further complexity. The identity of the atom occupying a particular site needs to be specified and information is also required on the chemical ordering and hence on how the concentration of a particular species varies across the network. Recent investigations show that the glassy phase has two characteristic length scales at distances larger than the nearest neighbour. One is associated with the intermediate range, and the other is associated with an extended range, which relates to a propagation of short range ordering [27].

Consider an ideal disordered network representing a binary oxide system such as amorphous SiO_2 or GeO_2 . The three-dimensional (3D) disordered network in these oxides is formed by $[\text{SiO}_4]$ or $[\text{GeO}_4]$ tetrahedra interconnected via bridging oxygens $\equiv \text{Si} \bullet \text{O} \bullet \text{Si} \equiv$, where \bullet designates a bond between Si and O, and $-$ designates a bridging oxygen atom with two bonds $\bullet \text{O} \bullet$. The ideal network can also contain some point defects in the form of broken bonds $\equiv \text{Si} \circ \text{O} \bullet \text{Si} \equiv$, where \circ designates a broken bond between Si and O. Each broken bond, which is typically associated with strain release and local adjustment of centres of atomic vibration, is treated as an elementary configurational excitation in the system of bonds and is termed a configuron [28]. Using Angell's bond lattice model we can represent condensed phases by their bond network structures [28, 29]. Thus we can focus our attention on temperature changes that occur in the system of interconnecting bonds of a disordered material rather than of atoms. In this approach the initial set of N strongly interacting cations such as Si^{4+} or Ge^{4+} is replaced by a congruent set of weakly interacting bonds of the system. The number of bonds will be $N_b = NZ$ where Z is the coordination number of cations, e.g. $Z = 4$ for SiO_2 and GeO_2 . For amorphous materials which have no bridging atoms such as oxygen in SiO_2 and GeO_2 or chlorine in ZnCl_2 , i.e. for amorphous Fe or Ge, $N_b = NZ/2$. Figure 1 illustrates the replacement of atomic structure by the congruent bond structure being either

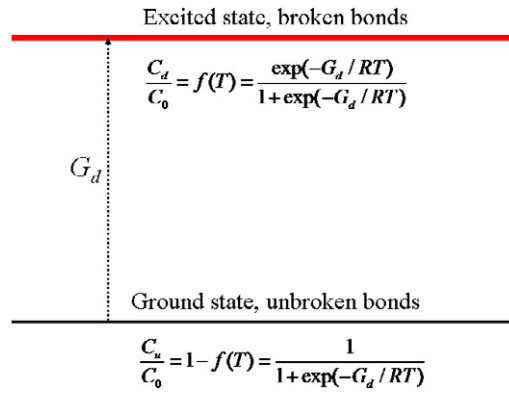


Figure 2. Two-level state equivalent to disordered system of bonds of an amorphous material.

unbroken or broken for amorphous silica when one of four Si•O bonds in the configurational [SiO₄] tetrahedron is broken.

At absolute zero temperature $T = 0$ the material network contains no broken bonds; however, at any finite temperature T the network contains thermally activated defects, e.g. configurons. Compared with a crystal lattice of the same material, the disordered network typically contains significantly more point defects such as broken bonds or vacancies. For example, the relative concentration of vacancies in crystalline metals just below the melting point is only 10^{-3} – 10^{-4} [3, 30]. The energetics of the disordered net are weaker and point defects can be formed more easily than in crystals of the same chemical composition. The difference arises from the thermodynamic parameters of defects in disordered networks. Nonetheless since they are metastable the amorphous materials can be well described by traditional thermodynamic methods [6, 11–15, 31]. The formation of defects in a network is governed by the formation Gibbs free energy $G_d = H_d - TS_d$, where H_d is the enthalpy and S_d is the entropy of formation of network defects, e.g. broken Si•O or Ge•O bonds. Recently, Doremus suggested that diffusion of silicon and oxygen in silicate melts takes place by transport of defect SiO molecules formed in the melt [22]. Formation of these defects occurs via breaking of covalent Si•O bonds and attachment of additional oxygen atoms which leads to five-coordination of oxygen atoms around silicon. Supporting experimental evidence for five-coordination of silicon and oxygen has been found in silicates [22].

Temperature-induced formation of network-breaking defects in a disordered network can be represented by the reaction involving the breaking of a covalent bond, e.g. in amorphous silica:



The higher the temperature the higher the concentration of thermally created defects such as broken bonds or configurons. Because the system of bonds has two states, namely the ground state corresponding to unbroken bonds and the excited state corresponding to broken bonds, it can be described by the statistics of two-level systems. Two states of the equivalent system (figure 2) are separated by the energy interval G_d governing the reaction (1).

The statistics of two-level systems leads to the well-known relationship for equilibrium concentrations of configurons C_d and unbroken bonds C_u [8, 23, 24, 28, 29]

$$C_d = C_0 f(T), \quad C_u = C_0 [1 - f(T)], \quad f(T) = \frac{\exp(-G_d/RT)}{1 + \exp(-G_d/RT)} \quad (2)$$

where C_0 is the total concentration of elementary bond network blocks or the concentration of unbroken bonds at absolute zero temperature $C_u(0) = C_0$. These demonstrate that the concentration of configurons gradually increases with increase in temperature and at $T \rightarrow \infty$ achieves its maximum possible value $C_d = 0.5C_0$ when $G_d > 0$. To evaluate further the equilibrium concentration of defects in amorphous materials requires numerical values for H_d and S_d which can be calculated using density functional theory methods [32]. H_d can be approximated since it should be approximately equal to half of the bond strength which is the case for silica where the bond strength of silicon equals 443 kJ mol^{-1} [33] and $H_d \approx 220 \text{ kJ mol}^{-1}$ [24]. Due to the lower symmetry of disordered materials S_d can be expected to be higher than in a crystal lattice. Defect entropy plays an important role in crystalline materials due to the high entropy values and carrier concentrations and their high mobility in ionic conductors [34, 35]. We evaluate both H_d and S_d from experimentally measured viscosity data of amorphous materials based on Doremus' model of viscosity which relates the viscosity of net-forming materials to thermodynamic parameters of network defects [22–24].

3. Thermodynamic parameters from viscosity data

It has been demonstrated recently that the viscosity of amorphous materials is directly related to the thermodynamic parameters of network-breaking defects [22–24]. The generic form for the viscosity equation is

$$\eta(T) = A_1 T \left[1 + A_2 \exp\left(\frac{B}{RT}\right) \right] \left[1 + C \exp\left(\frac{D}{RT}\right) \right], \quad (3)$$

$$\begin{aligned} A_1 &= k/6\pi r D_0, & A_2 &= \exp(-S_m/R), & B &= H_m, \\ C &= \exp(-S_d/R), & D &= H_d, \end{aligned} \quad (3a)$$

where k is the Boltzmann constant, R is the molar gas constant, r is the radius of the configuron, $D_0 = f\alpha\lambda^2\nu$, f is the correlation factor, α is the symmetry parameter, λ is the configuron's jump distance, ν is the vibration frequency for a jumping configuron and S_m and H_m are the entropy and enthalpy of motion of configurons. This equation can be fitted to practically all available experimental data on viscosities of amorphous materials [23, 24]. Moreover equation (3) can be readily approximated within a narrow temperature interval by known empirical and theoretical models such as Vogel–Fulcher–Tamman, Adam–Gibbs or the Kohlrausch-type stretch-exponential law [22, 36, 37]. In contrast to such approximations, equation (3) can be used in wider temperature ranges and gives correct Arrhenius-type asymptotes of viscosity at high $\eta(T) \cong A_1 A_2 (1 + C) T \exp(B/RT)$ and low $\eta(T) \cong A_1 A_2 C T \exp[(B + D)/RT]$ temperatures. It shows also that at extremely high temperatures when $T \rightarrow \infty$ the viscosity of melts changes to a non-activated, e.g. non-Arrhenius type, behaviour $\eta(T) \xrightarrow{T \rightarrow \infty} A_1 (1 + A_2) (1 + C) T$ which is characteristic of systems of almost free particles [8]. Five coefficients A_1 , A_2 , B , C and D in equation (3) can be treated as fitting parameters derived from the experimentally known viscosity data. By use of relationships (3a), from the numerical data of fitting parameters one can evaluate the thermodynamic data of network-breaking defects such as configurons. Experiments show that in practice four fitting parameters suffice [38] and the viscosity is well described by a simplified version of equation (3): $\eta(T) = AT \exp(B/RT) [1 + C \exp(D/RT)]$. This equation follows from (3) assuming that $A_2 \exp(B/RT) \gg 1$ and accounting for $A = A_1 A_2$. Hence from known viscosity–temperature relationships of amorphous materials we can evaluate H_d , S_d and H_m to characterize the thermodynamics of configurons in the material's network [23].

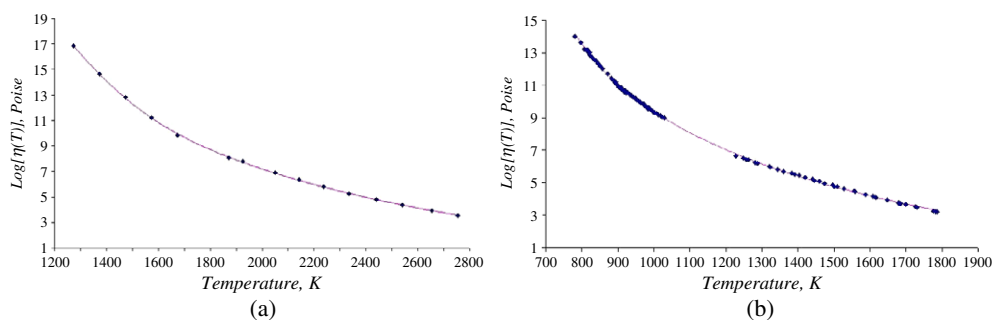


Figure 3. Viscosity–temperature relationships for amorphous (a) silica and (b) germania.

Table 1. Thermodynamic parameters of configurons in amorphous silica and germania.

| Amorphous oxide | H_d (kJ mol ⁻¹) | H_m (kJ mol ⁻¹) | S_d (R) |
|------------------|-------------------------------|-------------------------------|-----------|
| SiO ₂ | 220 | 525 | 16.13 |
| GeO ₂ | 129 | 272 | 17.84 |

An example of such an evaluation is demonstrated in figure 3, which shows viscosity–temperature relationships for amorphous silica and germania best fitted to theoretical curves. Experimental data for the viscosity of silica were taken from [39, 40] and for germania from [41]. Best fitted curves were calculated using equation (3) and as usual assuming that $A_2 \exp(B/RT) \gg 1$.

Figure 3 demonstrates the excellent agreement of theory with experiment with less than 0.5% deviation of calculated from measured data. Using relationships (3a) from the numerical data of fitting parameters A , B , C and D of equation (3) which provide the best fit of the theoretical viscosity–temperature relationship (3) to experimental data [39–41] we can evaluate the thermodynamic data of network-breaking defects in amorphous germania and silica (table 1).

The thermodynamic parameters from table 1 can be used to calculate viscosity–temperature relationships of amorphous silica and germania.

4. Geometry of disordered bonds network

Amorphous materials have an internal structure made of a more or less developed 3D network of interconnected structural blocks. Amorphous silica and germania are represented by 3D topologically disordered networks formed via N interconnected [SiO₄] or [GeO₄] tetrahedra through bridging oxygen atoms (figure 1). This disordered network is replaced by an equivalent disordered network made of $4N$ weakly interacting bonds which can be in two states either ground (unbroken) or excited (broken) (figure 2). The higher the temperature the higher the concentration of excited bonds; however, at absolute zero temperature all bonds are in the ground state. At temperatures close to absolute zero when $f(T) \rightarrow 0$ the concentration of excited bonds is very small so that these are homogeneously distributed in the form of single configurons in the disordered bond network. Motion of configurons in the bond network occurs in the form of thermally activated jumps from site to site and in this case all jump sites are equivalent in the network. The network thus can be characterized as an ideal 3D disordered structure which is described by a Euclidean 3D geometry. Its geometry remains 3D until the concentration of breaking defects is so low that we can neglect any clustering of configurons.

However, as the temperature increases due to reaction (1) the concentration of configurons gradually increases as follows from equation (2). The higher the temperature the higher the concentration of configurons and hence some of them will inevitably be in the vicinity of others. Two and more nearby configurons form clusters of configurons, and the higher the concentration of configurons the higher the probability of their clustering. The higher the temperature the larger are the clusters made of configurons in the disordered bond network. Finally, as is known from percolation theory, when the concentration of configurons exceeds the threshold level they form a macroscopic so-called percolation cluster, which penetrates the whole volume of the disordered network [26, 42]. As configurons are moving in the disordered network the percolation cluster made of broken bonds is a dynamic structure which changes its configuration, while remaining an infinite percolation cluster [24]. The percolation cluster is made entirely of broken bonds and hence is readily available for a more percolative than site-to-site diffusive motion of configurons. Hence above the percolation level the motion of configurons in the bond network occurs via preferred pathways through the percolation cluster. The percolation cluster is also called an infinite cluster as it penetrates the whole volume of material which as a result is expected to drastically change its physical properties from solid-like below to fluid-like above the percolation threshold [18, 21]. The geometry of a percolation cluster is fractal with the Hausdorff dimension $d_f = d - \beta/\nu$, where β and ν are critical exponents (indexes) and $d = 3$ is the dimension of the space occupied by the initial disordered network, so that $d_f = 2.55 \pm 0.05$ [26, 42]. Above the percolation threshold the disordered bond network can be characterized for moving configurons as a fractal disordered structure which is described by a fractal d_f -dimensional geometry. Hence when considering the motion of configurons in the disordered network their geometry is Euclidean 3D at low temperatures and low defect concentrations, whereas at high temperature when the broken bond concentration is above the percolation threshold it changes to a fractal one with Hausdorff dimension $d_f = 2.55 \pm 0.05$. The formation of a percolation cluster changes the topology of the bond network from Euclidean 3D below to the fractal d_f -dimensional above the percolation threshold.

An amorphous material is represented by a disordered bond network at all temperatures; however, it has a uniform 3D distribution of network-breaking defects at low concentrations in a glassy state and a fractal d_f -dimensional distribution at high enough temperatures when their concentration exceeds the percolation threshold in the liquid state. Changes that occur in the geometries of amorphous material at T_g affect their mechanical properties. Above T_g , as the geometry is fractal as in liquids [20], the mechanical properties are similar to those of liquids. The network of material remains disordered at all temperatures although the space distribution of configurons as seen above is different below and above the percolation threshold, changing the geometry from the Euclidean to fractal. Although to a certain extent being disordered at all temperatures the bond network above the percolation threshold becomes more ordered as a significant fraction of broken bonds belong to the percolation cluster.

Crystalline materials are characterized by 3D Euclidean geometries below their melting point T_m . Hence glasses below T_g and crystals below T_m are characterized by the same 3D geometry. Glasses behave like isotropic solids and are brittle. Because of the 3D bond geometry glasses are brittle materials which break abruptly and the fracture surfaces of glasses typically appear flat in the 'mirror' zone. It is known, however, that when analysed at the nanometre scale with an atomic force microscope they reveal a roughness which is similar to that exhibited by metallic fracture surfaces [43]. Glasses change their bond geometry at T_g . When melting occurs the geometry of crystalline materials also changes, as revealed by MD experiments, to fractal structure with $d_f \approx 2.6$ [20]. Table 2 summarizes the changes in the geometry of bond structures of both amorphous and crystalline structures.

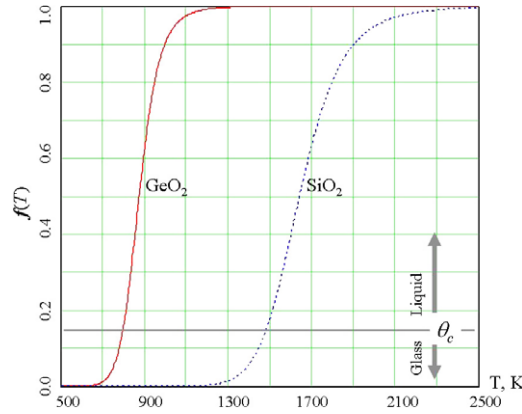


Figure 4. Relative concentration of configurons in amorphous silica and germania.

Table 2. Hausdorff dimensions of bond structures.

| Temperature | $0 < T < T_g$ | $T_g < T < T_m$ | $T > T_m$ |
|---------------------------------------|---------------|-----------------------|-----------|
| Amorphous material state | Solid | Liquid | |
| Hausdorff dimension of bond structure | $d = 3$ | $d_f = 2.55 \pm 0.05$ | |
| Crystalline material state | Solid | | Liquid |
| Hausdorff dimension of bond structure | $d = 3$ | $d_f \approx 2.6$ | |

5. Glass–liquid transition

As the bond network of an amorphous material is disordered the concentration of configurons at which the percolation threshold is achieved can be found using the universal critical percolation density θ_c , which remains the same for both ordered and disordered lattices [26, 42, 44]. The relative concentration of defects is given by $f(T) = C_d/C_0$ which shows that the higher the temperature the higher is $f(T)$. Assuming that at $C_d/C_0 = 1$ the space is completely filled by configurons we can designate $f(T)$ as the volume fraction of space occupied by randomly distributed configurons. Thus the critical temperature T_g at which the percolation level is achieved can be found assuming that the configurons achieve the universal critical density given by the percolation theory

$$f(T_g) = \theta_c. \quad (4)$$

For SiO_2 and GeO_2 we suppose that $\theta_c = \vartheta_c$ where ϑ_c is the Scher–Zallen critical density in 3D space $\vartheta_c = 0.15 \pm 0.01$ [26, 42, 44]. Note that for real percolating systems the value of θ_c can be significantly lower [26]. At temperatures above T_g the space is filled by configurons at concentrations which exceed the critical density θ_c , therefore they form the percolation cluster with fractal geometry changing the state of material from solid-like (glass) to liquid-like (figure 4).

Accounting for (2) from (4) we find that T_g is directly related to the configuron thermodynamic parameters via:

$$T_g = \frac{H_d}{S_d + R \ln[(1 - \theta_c)/\theta_c]}. \quad (5)$$

Below T_g the configurons are uniformly distributed in space and formation of clusters is improbable. The geometry of network defects in this area can be characterized as Euclidean.

Table 3. Glass transition temperatures (T_g) in amorphous SiO₂ and GeO₂.

| Amorphous oxide | SiO ₂ | GeO ₂ |
|---------------------------------|------------------|------------------|
| T_g , calculated from (5) (K) | 1482 | 792 |
| T_g , experiment [45, 46] (K) | 1475 | 786 |

With increase of temperature at $T = T_g$, the concentration of defects achieves the critical concentration for formation of a percolation cluster. Above T_g a percolation cluster made of network defects is formed and the geometry of the network becomes fractal. Hence at $T > T_g$ amorphous materials can be considered as supercooled liquids. We expect that T_g obtained from (5) will have values close to those experimentally observed. Table 3 gives T_g calculated using equation (5) and experimentally measured data on transition from the glassy to the supercooled liquid state (e.g. temperatures when the supercooled liquid state is reached) from [45, 46].

The agreement between calculated and experimentally measured data on transition from the glassy to the supercooled liquid state is excellent: calculated values of T_g , which are entirely based on processing of continuous viscosity–temperature relationships taken from earlier works [18, 19], nearly coincide (within 0.5–0.7%) with recently measured calorimetric T_g [45, 46].

Although the formation of glass is a kinetically controlled process, equation (5) demonstrates that T_g is a thermodynamic parameter of an amorphous materials and its network-breaking defects (configurons) rather than a kinetic or dynamic one. It is worth noting that taking into account $S_d \gg R$ we can simplify equation (5) to an approximation similar in form to the well-known Dienes ratio [35, 47] $T_g \approx H_d/S_d$. In addition equation (5) conforms well to Hunt's equation for T_g of ionic glasses $T_g \approx E_m/18k$, where E_m is the peak hopping energy barrier [48]. This can be seen by noting that the hopping barrier can be assessed as $E_m = H_d/N_A$, where N_A is Avogadro's number, e.g. for amorphous silica equation (5) gives $T_g \approx H_d/18R$ which is almost the same as given by Hunt's equation.

6. The role of kinetics

We obtained the temperature of transition from a glassy to a supercooled liquid state (5) without considering the formation of crystalline phases. Changes at the glass transition are kinetically controlled and occur when the cooling rate is so high that crystallization is negligible. A liquid is always in a metastable state below its melting point (T_m), thus whether it becomes a glass or a crystal depends critically on cooling rate. When the cooling rate is slow any liquid crystallizes, except atactic polymers that hardly crystallize due to stereoirregularity [1]. A liquid always tends to crystallize into the equilibrium crystal. The tendency to crystallize is well expressed by the fragility of melts, which Angell suggested is used to describe the deviation of viscosity from Arrhenius-type behaviour [49]. This deviation is caused by changes in the activation energies of viscosity and enables numerical characterization of the fragility via Doremus' criterion of fragility $R_D = 1 + H_d/H_m$, where H_m is the enthalpy of motion of configurons [23, 24]. Strong network liquids such as SiO₂ and GeO₂ are well polymerized, mostly covalently bonded, and demonstrate a nearly Arrhenius temperature dependence of viscosity. These have small values of R_D : SiO₂, has $R_D = 1.42$ and GeO₂ has $R_D = 1.33$ [22, 24]. In contrast the activation energies of fragile liquids change significantly with temperature so their viscosity deviates significantly from the Arrhenius behaviour. Typical fragile glass-forming liquids are chalcogenides or iron phosphates, whose networks are mostly ionic. These are characterized

by large values of $R_D \gg 1$ (diopside has $R_D = 7.26$ [50]). Fragility of amorphous materials is reflected by a high sensitivity of the melt viscosity to temperature and by a strong tendency to crystallize. It is known that when a fragile material is heated or cooled at a normal rate, say 20 K min^{-1} , the exothermic peaks due to crystallization processes can be easily detected using a differential scanning calorimeter. Moreover, experiments with fragile basalt systems reveal ordered structures even above the liquidus temperature [51]. Large-scale density fluctuations, known as Fischer clusters, commonly exist in fragile liquids and are revealed in one-component glass-forming liquids and polymers [52]. Bakai [53] showed that the observed fluctuations appear as a result of aggregation of liquid domains, and developed the idea that a glass-forming liquid has a heterophase mesoscopic structure consisting of solid-like and fluid-like species. In contrast strong liquids are more difficult to crystallize than fragile ones below T_g since their kinetics are almost controlled by α -relaxation [1]. Hence equation (5) is readily applicable to calculating T_g for strong liquids and at relatively fast cooling rates.

A certain amount of crystalline phase inevitably forms when a glass is formed via cooling a liquid. The lower the cooling rate, q , the higher the volume fraction, x , occupied by crystalline phases. Finally, at very low cooling rates when q is below the critical cooling rate $q_c(x_c)$ formation of glass is impeded by crystallization. The critical cooling rate is defined as the lowest cooling rate at which the final degree of crystallinity of amorphous material does not exceed a given critical value x_c , which can be close to unity when the glass crystallizes. For good glass-forming liquids x_c is normally assumed to be within 10^{-6} – 10^{-2} [54, 55]. The volume fraction of crystallized material can be found in the framework of the Kolmogorov–Avrami theory of phase transformations. It can be expressed in the simplest case of a constant nucleation rate per unit volume, I_v , as an integral function at constant cooling rate q [55–57]: $x = 1 - \exp(-\pi I_v u^3 t^4/3)$ where t is time and u is the rate of growth of the crystalline phase. Note that nucleation rates are at a maximum near T_g [57] which emphasizes the role of crystallization at the liquid–glass transition [1]. The fraction of crystalline phase is proportional to q^{-4} or t^4 : $x \cong \pi I_v u^3 t^4/3$ when $x \ll 1$. Generally, the higher the cooling rate q the smaller is x . The actual volume of vitreous phase hence depends on cooling rate and can be expressed as $x_g = 1 - x$. At finite cooling rates the actual volume of amorphous material available for the formation of percolation clusters made of configurons is lower. This reduction can be accounted for in the equation for critical temperature of percolation including a renormalization term in (4) $f(T_g) = \theta_c x_g = \theta_c(1 - x)$. Thus when taking into account the formation of crystalline phases we obtain a renormalized equation for T_g :

$$T_g = \frac{H_d}{S_d + R \ln[(1 + x - \theta_c)/\theta_c]}. \quad (6)$$

This shows that when $x \ll 1$ T_g increases logarithmically with q :

$$T_g = H_d/[S_d + R \ln[[1 - \theta_c + \pi I_v (T_m - T_g)^4 u^3/3q^4]/\theta_c]]$$

and achieves its maximum value given by (5) at $q \rightarrow \infty$ when the volume fraction of crystalline material is negligibly low so $x \rightarrow 0$. T_g diminishes with the diminution of q , although its reduction is limited by formation of crystalline phases as when $q \rightarrow 0$ the fraction of crystalline material $x \rightarrow 1$. Thus at very low cooling rates the vitreous phase is hardly formed as the only phase formed is crystalline. The interval of temperatures where the glass transition occurs can be assessed from (6) taking into account that there is a minimum possible cooling rate q_{\min} or correspondingly a maximum cooling time t_{\max} when a glass can be obtained via cooling. The minimum possible cooling rate q_{\min} and corresponding maximum cooling time t_{\max} are found considering the crystallization kinetics [54, 55]. This gives for the glass transition interval $\Delta T_g \approx T_g(R/S_d) \ln(5.66 + 0.39\pi I_v u^3 t_{\max}^4)$ which reproduces the experimentally known logarithmic behaviour of T_g with cooling rate [6, 58]. Although the glass transition

temperature is a thermodynamic parameter it depends on the cooling rate of a supercooled liquid as the formation of glass is a kinetically controlled process. The T_g s of amorphous materials achieve their maximum thermodynamic values at infinitely high cooling rates.

7. Derivative discontinuities

The concentration of configurons changes continuously with temperature, therefore no discontinuities are expected to occur at T_g for integral properties of amorphous materials. MD simulations show that derivative characteristics such as specific heat demonstrate discontinuities at T_g [17, 18]. The discontinuities are explained by accounting for the formation of percolation clusters and the change in the geometry of distribution of configurons. The characteristic linear scale which describes the branch sizes of clusters formed by configurons is the correlation length $\xi(T)$. It gives the linear dimension above which the material is homogeneous and can be characterized as a material with uniformly distributed configurons. Because of the formation of percolation clusters at lengths smaller than $\xi(T)$ the material has a fractal geometry [42]. At temperatures approaching T_g the correlation length ξ diverges: $\xi(T) = \xi_0/|f(T) - \theta_c|^\nu$, where the critical exponent $\nu = 0.88$ [26, 42]. Accounting for this we can describe finite size effects in the glass transition where a drift to higher values of T_g is observed when sample sizes L diminishes: $T_g(\infty) - T_g(L) \sim 1/L$ [59, 60]. Indeed assuming that the glass–liquid transition is achieved when the correlation length is equal to the size of sample $\xi(T) = L$ we obtain $T_g(\infty) - T_g(L) = 0.1275T_g(RT_g/H_d)(\xi_0/L)^{1.136}$ which conforms well to Hunt’s conclusions [59, 60].

Following approaches developed in Angell’s bond lattice model [28, 29] we can find the heat capacity per mole of configurons involved in the percolation cluster near T_g :

$$C_{p,\text{conf}} = R \left(\frac{H_d}{RT} \right)^2 f(T)[1 - f(T)] \left(1 + \beta P_0(\Delta H/H_d) \frac{T_1^{1-\beta}}{|T - T_g|^{(1-\beta)}} \right) \quad (7)$$

where $T_1 = RT_g^2/\theta_c(1 - \theta_c)H_d$, P_0 is a numerical coefficient close to unity (for strong liquids $P_0 = 1.0695$) and $\Delta H \ll H_d$ is the enthalpy of bonding of configurons in the percolation cluster. ΔH can be found by accounting for the fact that the enthalpy of formation of one mole of configurons which belong to a percolation cluster H_c is higher than H_d , e.g. $\Delta H = H_c - H_d$. Thus the configurons in a percolation cluster are not condensed in a condensed excited state, which makes it different from Holmlid’s clusters where $\Delta H < 0$ [61, 62]. From (7) one can see that the heat capacity shows a divergence near $T_g \propto 1/|T - T_g|^{0.59}$. Because $T_1 \ll T_g$ with further increase of temperature the divergence observed at T_g becomes negligible and the contribution of (7) to the heat capacity of an amorphous material is insignificant, which is consistent with experimental observations [63, 64]. Figure 5 illustrates this type of behaviour for the specific heat of *o*-terphenyl near the glass transition.

Thus the glass transition shows typical features of second order phase transformations including universal behaviour near the phase transition temperature [8]. From (7) we can find that the universal critical exponent at the glass transition $\alpha = 0.59$.

8. Conclusions

We analysed the disordered structure of bonds and the geometry of the spatial distribution of configurons (thermal equilibrium network-breaking defects in a network of bonds) of an amorphous material. Amorphous SiO_2 and GeO_2 were used as simple glass-forming materials for this purpose. Thermodynamic data for broken bonds were evaluated based on viscosity–temperature relationships and Doremus’ defect model of viscosity. Evaluation of configuron

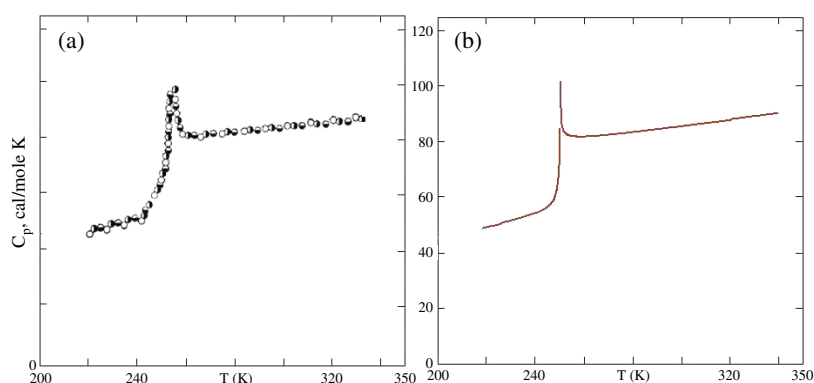


Figure 5. Specific heat of amorphous *o*-terphenyl: (a) experimental data from [61, 62]; (b) calculated curves accounting for contribution (7).

concentration revealed temperature ranges where dynamic percolation clusters made of broken bonds are formed. We defined T_g as the temperature where a percolation cluster made of configurons is formed and found an excellent agreement between calculated and experimentally measured calorimetric T_g . We characterized the symmetry of topologically disordered systems by the Hausdorff dimension, d , of bonds. Our analysis revealed two types of topological disorder characterized by different symmetries below and above the T_g : (i) $d =$ three-dimensional (Euclidean), which occurs in the glassy state at $T < T_g$ when no percolation clusters are formed and (ii) $d_f = 2.55 \pm 0.05$ -dimensional (fractal), which occurs in the liquid state at $T > T_g$ when percolation clusters made of broken bonds are formed. Our results are hence consistent with previous work and reflect the same change in geometry of the distribution of atoms in amorphous materials at T_g . Thus the transition from a glassy to a supercooled liquid state can be treated as a change in the symmetry of topological disorder.

Acknowledgments

The authors acknowledge useful discussions with L Holmlid, A Hunt and V Stolyarova.

References

- [1] Tanaka H 2005 *J. Non-Cryst. Solids* **351** 3371–84
- [2] Binder K and Young A P 1986 *Rev. Mod. Phys.* **58** 801–976
- [3] Kittel C 1996 *Introduction to Solid State Physics* (New York: Wiley)
- [4] Richert R 2002 *J. Phys.: Condens. Matter* **14** R703–38
- [5] Roland C M and Casalini R 2005 *J. Non-Cryst. Solids* **351** 2581–7
- [6] Zarzycki J 1982 *Glasses and the Vitreous State* (New York: Cambridge University Press)
- [7] 1997 *IUPAC Compendium Chem. Terminol.* **66** 583
- [8] Landau L D and Lifshitz E M 1984 *Statistical Physics* Part 1 (Butterworth: Heynemann)
- [9] Hunt A 1992 *Solid State Commun.* **84** 263–6
- [10] Gutzow I and Petroff B 2004 *J. Non-Cryst. Solids* **345/346** 528–36
- [11] Doremus R H 1973 *Glass Science* (New York: Wiley)
- [12] Zallen R 1983 *The Physics of Amorphous Solids* (New York: Wiley)
- [13] Ziman J M 1979 *Models of Disorder* (Cambridge: Cambridge University Press)
- [14] Debenedetti P G 1997 *Metastable Liquids* (Princeton, NJ: Princeton University Press)
- [15] Donth E 2001 *The Glass Transition* (Berlin: Springer)
- [16] Hobbs L W 1995 *J. Non-Cryst. Solids* **192/193** 79–91

- [17] Medvedev N N, Geider A and Brostow W 1990 *J. Chem. Phys.* **93** 8337
- [18] Evtsev A V, Kosilov A T and Levchenko E V 2002 *JETP Lett.* **76** 104
- [19] Binder K 2000 *J. Non-Cryst. Solids* **274** 332
- [20] Kolokol A S and Shimkevich A L 2005 *At. Energy* **98** 187–90
- [21] Ojovan M I 2004 *J. Exp. Theor. Phys. Lett.* **79** 632–4
- [22] Doremus R H 2002 *J. Appl. Phys.* **92** 7619–29
- [23] Ojovan M I and Lee W E 2004 *J. Appl. Phys.* **95** 3803–10
- [24] Ojovan M I and Lee W E 2005 *Phys. Chem. Glasses* **46** 7–11
- [25] Ozhovan M I 1993 *J. Exp. Theor. Phys.* **77** 939–43
- [26] Sahimi M 1994 *Applications of Percolation Theory* (London: Taylor and Francis)
- [27] Salmon P S, Martin R A, Mason P E and Cuello G J 2005 *Nature* **435** 75–7
- [28] Angell C A and Rao K J 1972 *J. Chem. Phys.* **57** 470–81
- [29] Angell C A and Wong J 1970 *J. Chem. Phys.* **53** 2053–66
- [30] Kraftmaker Y 1998 *Phys. Rep.* **299** 799
- [31] Sciortino F and Tartaglia P 2001 *Phys. Rev. Lett.* **86** 107–10
- [32] Chelikovsky J R and Louie S G 1996 *Quantum Theory of Real Materials* (Boston, MA: Kluwer)
- [33] Pavlushkin N M 1979 *Basics of Glassceramic Technology* (Moscow: Stroizdat)
- [34] Harding J H 1985 *Phys. Rev. B* **32** 6861
- [35] Almond D P and West A R 1987 *Solid State Ion.* **23** 27
- [36] Avramov I 2000 *J. Non-Cryst. Solids* **262** 258
- [37] Avramov I 2005 *J. Non-Cryst. Solids* **351** 3163–73
- [38] Volf M B 1988 *Mathematical Approach to Glass* (Amsterdam: Elsevier)
- [39] Urbain G, Bottinga Y and Richert P 1982 *Geochim. Cosmochim. Acta* **46** 1061
- [40] Hetherington G, Jack K H and Kennedy J C 1964 *Phys. Chem. Glasses* **5** 130
- [41] Fontana E H and Plummer WA 1966 *Phys. Chem. Glasses* **7** 139–46
- [42] Isichenko M B 1992 *Rev. Mod. Phys.* **64** 961
- [43] Celarie F, Prades S, Bonamy D, Ferrero L, Bouchaud E, Guillot C and Marliere C 2003 *Phys. Rev. Lett.* **90** 075504
- [44] Scher H and Zallen R 1970 *J. Chem. Phys.* **53** 3759
- [45] Bruning R 2003 *J. Non-Cryst. Solids* **330** 13–22
- [46] Bruning R and Crowell T 1999 *J. Non-Cryst. Solids* **248** 183–93
- [47] Dienes G C 1950 *J. Appl. Phys.* **21** 1189–92
- [48] Hunt A 1994 *J. Non-Cryst. Solids* **176** 288–93
- [49] Angell C A 1988 *J. Phys. Chem. Solids* **49** 863–71
- [50] Doremus R H 2003 *Am. Ceram. Soc. Bull.* **82** 59–63
- [51] Yue Y 2004 *J. Non-Cryst. Solids* **345/346** 523–7
- [52] Fischer E W, Meier G, Rabenau T, Patkowski A, Steffen W and Thonnes W 1991 *J. Non-Cryst. Solids* **131–133** 134
- [53] Bakai A S 2002 *J. Non-Cryst. Solids* **307–310** 623–9
- [54] Uhlmann D R 1972 *J. Non-Cryst. Solids* **7** 337
- [55] Avramov I, Zannotto E D and Prado M O 2003 *J. Non-Cryst. Solids* **320** 9
- [56] Uhlmann D R, Hays J F and Turnbull D 1966 *Phys. Chem. Glasses* **7** 159–68
- [57] Granasy L and James P F 1999 *J. Non-Cryst. Solids* **253** 210
- [58] Klinger M I 1988 *Phys. Rep.* **165** 275
- [59] Hunt A 1994 *Solid State Commun.* **90** 527–32
- [60] Hunt A 1996 *J. Non-Cryst. Solids* **195** 293–303
- [61] Holmlid L 2002 *J. Phys.: Condens. Matter* **14** 13469–79
- [62] Akesson H, Badiei S and Holmlid L 2006 *Chem. Phys.* **321** 215–22
- [63] Gotze W and Sjogren L 1992 *Rep. Prog. Phys.* **55** 241–376
- [64] Greed R J and Turnbull D 1967 *J. Chem. Phys.* **47** 2185–90